Journal of
Low Power Electronics and Applications

MDPI

Communication

First Review of Conductive Electrets for Low-Power Electronics

D. D. L. Chung

Composite Materials Research Laboratory, Department of Mechanical and Aerospace Engineering, The State University of New York, Buffalo, NY 14260-4400, USA; ddlchung@buffalo.edu

Abstract: This is the first review of conductive electrets (unpoled carbons and metals), which provide a new avenue for low-power electronics. The electret provides low DC voltage (μV) while allowing low DC current (μA) to pass through. Ohm's Law is obeyed. The voltage scales with the inter-electrode distance. Series connection of multiple electret components provides a series voltage that equals the sum of the voltages of the components if there is no bending at the connection between the components. Otherwise, the series voltage is below the sum. Bending within the component also diminishes the voltage because of the polarization continuity decrease. The electret originates from the interaction of a tiny fraction of the carriers with the atoms. This interaction results in the charge in the electret. Dividing the electret charge by the electret voltage V' provides the electret-based capacitance C', which is higher than the permittivity-based capacitance (conventional) by a large number of orders of magnitude. The C' governs the electret energy ($1/2\ C'V'^2$) and electret discharge time constant (RC', where R = resistance), as shown for metals. The discharge time is promoted by a larger inter-electrode distance. The electret discharges occur upon short-circuiting and charge back upon subsequent opencircuiting. The discharge or charge of the electret amounts to the discharge or charge of C'.

Keywords: electret; power source; low-power electronics; conductor; discharge; charge; graphite; metal; capacitance; permittivity

Citation: Chung, D.D.L. First Review of Conductive Electrets for Low-Power Electronics. *J. Low Power Electron. Appl.* **2023**, *13*, 25. https://doi.org/10.3390/jlpea13020025

Academic Editor: Andrea Acquaviva

Received: 10 February 2023
Revised: 23 March 2023
Accepted: 4 April 2023
Published: 6 April 2023

1. Low-Power Electronics

Low-power electronics for low-power-consumption analog and digital circuits and low-power data storage and processing are receiving increasing attention. There are numerous electronic functionalities, including swing field effect transistor devices, non-volatile memory, memristors, logic device, electronic skin, sensors, medical monitoring systems, electronic displays, and neuromorphic computing. The growth of low-power electronics is partly fueled by the reduction in power requirements for working electronic and energy systems (including portable and wearable electronics), as enabled by improved efficiency and component size reduction. It is also fueled by the growing demand for the "Internet-of-Things" (IoT).

Materials or devices that are exploited for low-power electronics include two-dimensional spintronics [1], graphene [2,3], soft microbial fuel cells [4], thermoelectrics [5], semiconductors [6], transition metal dichalcogenides [7], antiferroelectric-like materials in $HfZrO_2$ [8], piezoelectric nanogenerators [9], transition metal carbide/nitride (MXenes) [10], organic electronics [11], micro-supercapacitors [12], gallium selenide nanosheets [13], monolayer MoS_2 [14], negative-capacitance field effect transistors [15], TiO_2 nanofiber electrodes [16], ultrathin polymer insulating layers [17], organic conductor–elastomer-metal nanoparticles [18], organic solar cells [19], HfN_2 monolayers [20], triboelectric energy harvesters [21], RF energy harvesting systems [22], iontronic cellulose nanopaper [23], amorphous indium oxide with tantalum pentoxide [24], and dielectric tantalum pentoxide [25]. In particular, graphene in the form of heterostructures (with graphene used in combination with semiconductors or other layered two-dimensional materials) [2] or electrodes [3] has been

used. An electrode is not a power-providing component but is part of a material system for providing power.

2. Electret

An electret signifies a material that exhibits a permanent electric dipole. The electret behavior is a part of the dielectric behavior. It has historically been reported for nonconductors, particularly polymers and ceramics that have been poled [26–31], and has been exploited for microphones and other devices [32–46]. The poling process entails the application of a strong electric field [47–56]. It is disadvantageous in the tendency to depole after the poling and the consequent need to repole. Electrets in the form of conductors (particularly those without poling) are emerging (since 2019), as reported for flexible graphite [57], polycrystalline graphite [58], carbon fibers [59], carbon fiber composites [60], steel [61] and Sn-4Ag [62], all without poling.

Because of the lack of conductivity, the electrets involving nonconductors functioning as capacitors, with DC electric current being not able to flow through them continuously, though a DC pulse can flow in the direction from the positive electrode to the negative electrode (Figure 1a). On the other hand, electrets that are conductors function as resistors (Figure 1b), with continuous DC flow being feasible. With the provision of both DC voltage and DC, the conductive electret serves as a power source, which is enabled by the electret and conductive behavior of a conductor. This concept is new in the field of low-power electronics. This work is directed at providing the first review of the emerging subject of conductive electrets for low-power electronics.

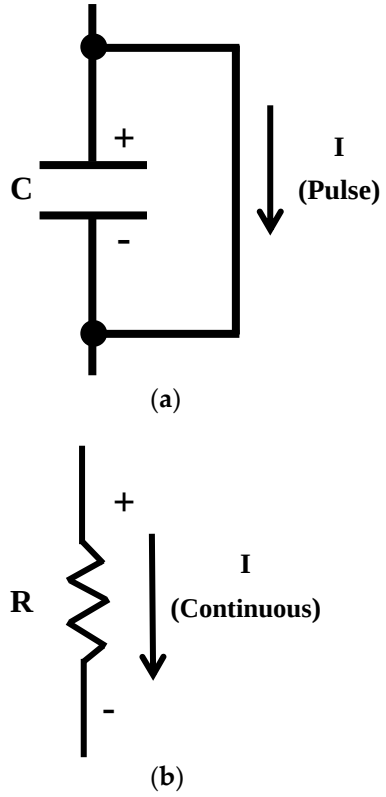

Figure 1. Models for describing the electrical behavior of electrets. C indicates the capacitor. R indicates the resistor. I indicates the current. (**a**) An electret that is a nonconductor. (**b**) An electret that is a conductor.

Graphite differs from the abovementioned graphene [2,3] in terms of its large number of carbon layers and its wide availability in various bulk forms. Graphite is widely used for heating elements and electrochemical electrodes [63–79], but its electret behavior is only

emerging [57,58]. Because of the electret behavior, graphite is a power-providing material in the absence of semiconductors or other two-dimensional materials, which are used in prior work on graphene [2]. Comparison of graphite with various grain sizes indicates that both the electric field in the electret and the electrical resistivity increase slightly as the grain size decreases [58].

3. Scientific Origin

The basic science is different from that of all previously reported power sources. Vibrations are not a mechanism for the energy generation of conductive electrets, although they are a mechanism in the case of nonconductive electrets. The nonconductive electrets behave as capacitors, whereas the conductive electrets behave as polarizable conductors (Figure 1). The mechanism for energy generation is described below for conductive electrets.

The permittivity is the key material property that describes the dielectric behavior. For a conductor, the permittivity originates from the interaction of a tiny fraction of the carriers with the atoms. As shown for graphite, the permittivity increases with the inverse of the grain size linearly [58]. This implies that the carrier-atom interaction occurs at the grain boundaries. The relative permittivity reaches 10^6 [80,81]. This is consistent with the "Giant polarizability" predicted theoretically for conductors by Jonscher (1922–2005) in 1999 [82].

An electret discharges by short-circuiting, and charges back upon subsequent open circuiting (Figure 2). The fact that discharge occurs without the need for a prior charge is expected from the fact that the electret does not require poling. In fact, poling enhances the electret negligibly [83]. In other words, the dipole in the electret is inherent (thermodynamically stable). The greater the inter-electrode distance, the longer the discharge time [58]. The discharge/charge of an electret involves that of capacitance. This capacitance is not the well-known capacitance that relates to permittivity but is a novel type of capacitance known as the electret-based capacitance [84]. In contrast to the permittivity-based capacitance, the electret-based capacitance is defined as the magnitude of the electret charge (determined by integrating the curve of discharge current concerning the time for the entire discharge period (Figure 2) divided by the electret voltage V'. The electret-based capacitance C' is higher than the permittivity-based capacitance C by numerous orders of magnitude [84]. For example, for Sn-4Ag lead-free solder, C' is 620 F, whereas C is only 175 pF [84]. The time constant of the discharge/charge approximately equals RC' (R = resistance) and the energy of the discharge/charge approximately equals $\frac{1}{2}\,C'V'^2$, as shown for metals [84].

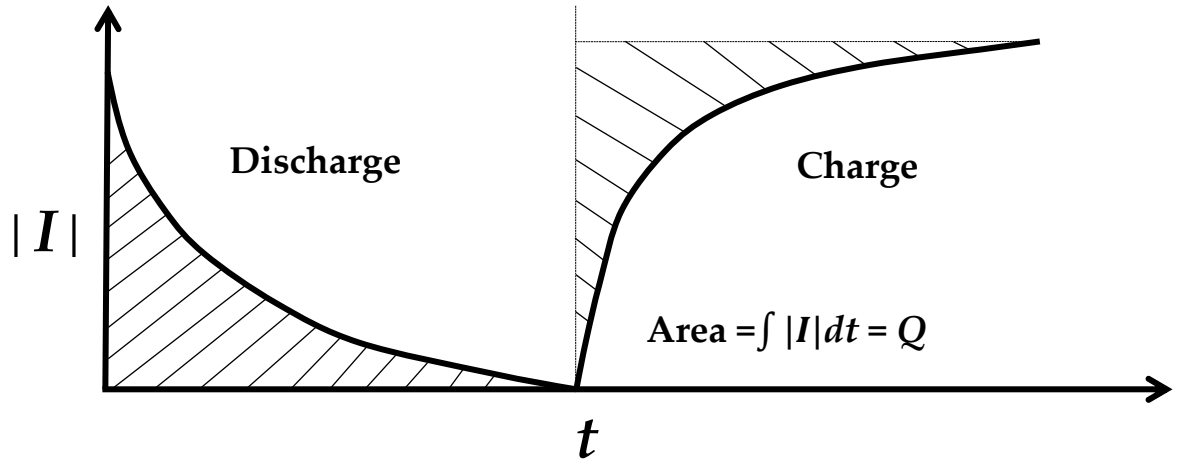

Figure 2. The discharge–charge behavior, as illustrated by the curve of the current magnitude ($|I|$) as a function of time (t) during discharge (short-circuited) and the subsequent charge (open-circuited). The shaded area gives the magnitude of charge Q associated with the discharge/charge.

The fraction of carriers that interact with the atoms is much greater for the electret (DC) than the permittivity (AC polarization) [58]. For graphite (grain size 1 μm), the fraction of

carriers that take part in the permittivity reaches 1.2×10^{-9}, while the fraction of carriers that take part in the electret discharge reaches 6.4×10^{-3} [58].

A conductor functions as a resistor with low-resistance (mΩ) (usual function), a capacitor with low-capacitance (pF, permittivity-based), and a power source that provides low voltage (μV, electret-based) [85]. The extent of a function compared to the other functions depends on the dimensions. For a given value of the cross-sectional area A, increasing the length (the inter-electrode distance l) increases the voltage V' while reducing the capacitance C (such that the capacitors are in series). For a given value of l, increasing A promotes C while reducing the resistance [85].

4. Electret Power Source Behavior

Flexible graphite is made by compacting graphite particles in the form of exfoliated graphite without a binder and is commercially available in the form of large sheets (Figure 3) [86–94]. Exfoliated graphite is expanded intercalated graphite, such that it has a cellular structure (Figure 4). The expansion is typically conducted by rapid heating of the intercalated graphite. Because of the cellular structure, multiple pieces of exfoliated graphite, with each piece made from a graphite flake, join by mechanical interlocking without the need for a binder.

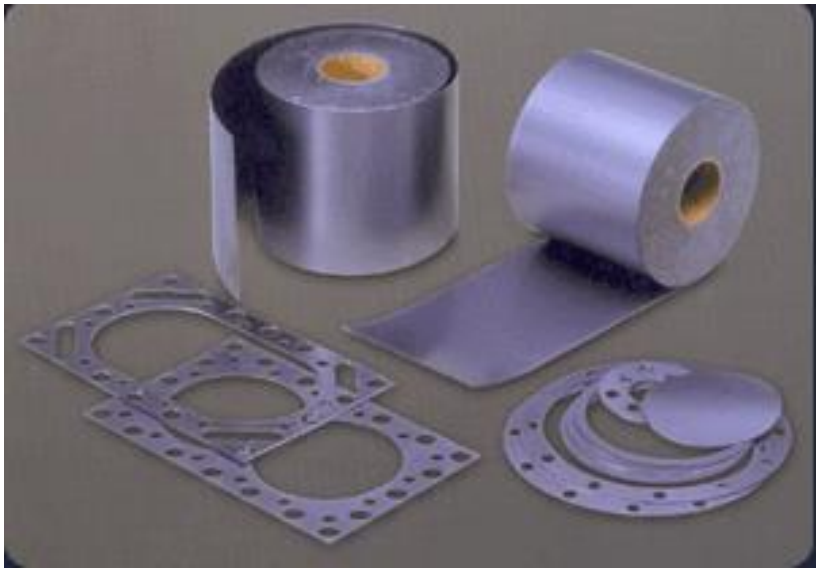

Figure 3. Flexible graphite commercially made by compacting particles of exfoliated graphite. http://www.mvivek.com/flexible.htm (public domain) (accessed on 5 April 2023).

The greater the inter-electrode distance, the longer the discharge time [58], as mentioned in Section 3. Presumably due to the microstructure, flexible graphite in the form of large sheets (hence making large inter-electrode distances feasible) exhibits a discharge time that is so long that the electret essentially does not discharge upon short-circuiting. Thus, this material is particularly suitable for use as a power source and its electret characteristics [95] are described below.

The electret voltage (Table 1) can be increased by a series connection of multiple pieces of the electret. The voltage is doubled when two essentially identical specimens are connected in series without bending the electrical connection between the two specimens, but the series voltage is roughly reduced by 50% when the electrical connection is bent [95]. This is indicated by comparing the case of an unbent connection (a silver-paint butt joint) (Figure 5) and the case of a bent connection (in the form of aluminum foil attached to the specimen by using silver paint) (Figure 6). The former gives a voltage that corresponds to the sum of the voltages of the two specimens that are disconnected from one another, but the latter gives a voltage that is less than the sum (Table 2).

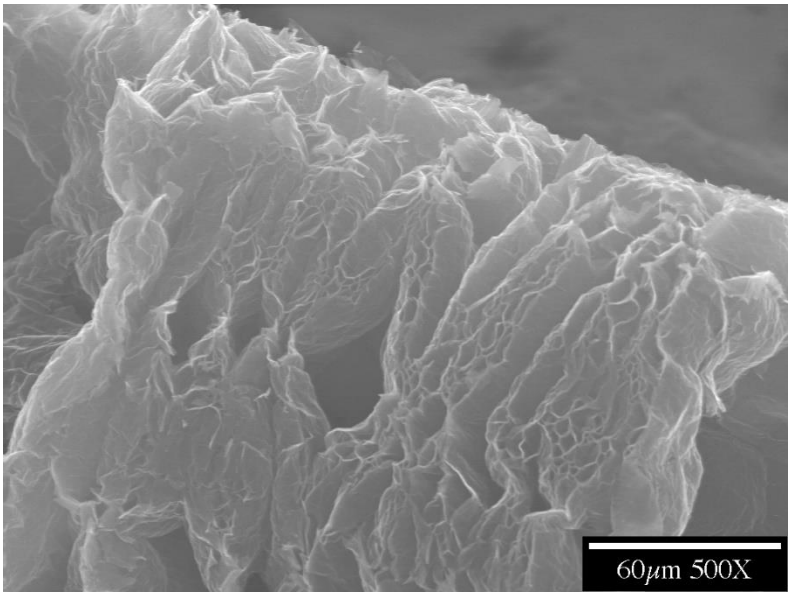

Figure 4. A part of a piece of exfoliated graphite, as made by the expansion of intercalated graphite. The cellular structure is shown.

Table 1. Electrical characteristics of electret in the form of flexible graphite (specimens labeled S1 and S2). The S1 + S2 column gives the sum of the values for S1 and S2 when these two specimens are not connected electrically. The electric field is obtained by dividing the voltage by the inter-electrode distance [95].

	S1	S2	S1 + S2 (Sum)
Dimensions (mm)	683 × 302 × 1.656	680 × 300 × 1.668	/
Inter-electrode distance (mm)	633 ± 0.5	630 ± 0.5	1313 ± 2
Resistance * (mΩ)	14.69 ± 0.12	14.08 ± 0.12	28.77 ± 0.24
Resistivity (10^{-5} Ω.m)	1.16 ± 0.02	1.12 ± 0.02	/
Voltage before polarity reversal (μV)	+1.139 ± 0.010	+1.145 ± 0.005	+2.284 ± 0.015
Voltage after polarity reversal (μV)	−0.961 ± 0.009	−1.109 ± 0.007	−2.070 ± 0.016

* Four-probe resistance.

Table 2. Effect of the bending of the series connection of two electrets (S1 + S2) in the form of flexible graphite. The electret voltage is compared for two cases, i.e., the case of no bending of the electrical connection and the case of bending of the connection. The two specimens (S1 + S2) positioned side by side are joined in a butt fashion at their edges. The inter-electrode distance corresponds to the distance between the proximate edges of the two voltage electrodes, with one electrode positioned close to the left end of the left specimen (S1) and the other electrode positioned close to the right end of the right specimen (S2) [95].

Specimens S1 + S2 Inter-Electrode Distance = 1313 ± 2 mm	Voltage (μV)		Fractional Change in Voltage Magnitude Relative to the Sum (%)		Electric Field (μV/m)	
	Before Polarity Reversal	After Polarity Reversal	Before Polarity Reversal	After Polarity Reversal	Before Polarity Reversal	After Polarity Reversal
Without bending in the connection *	+2.246 ±0.015	−2.105 ±0.011	−1.7 ±1.3	+1.7 ±1.3	+1.711 ±0.012	−1.603 ±0.009
With bending in the connection †	+1.054 ±0.027	−1.008 ±0.034	−53.9 ±1.9	−51.3 ±2.4	+0.803 ±0.021	−0.768 ±0.025
Sum of the voltages of two disconnected specimens	+2.284 ±0.015	−2.070 ±0.016	/	/	+1.740 ±0.012	−1.577 ±0.012

* For the case without connection bending, the butt joint is obtained by applying silver paint along the full length of the joint (Figure 5, for S1 + S2). † For the case with connection bending, the butt joint is obtained by applying a layer of double-sided adhesive tape along the full length of the joint. The two specimens (S1 + S2) are electrically connected via aluminum foil leads, with a lead protruding from each specimen. The protruded leads are connected by applying silver paint on the leads (Figure 6, for S1 + S2).

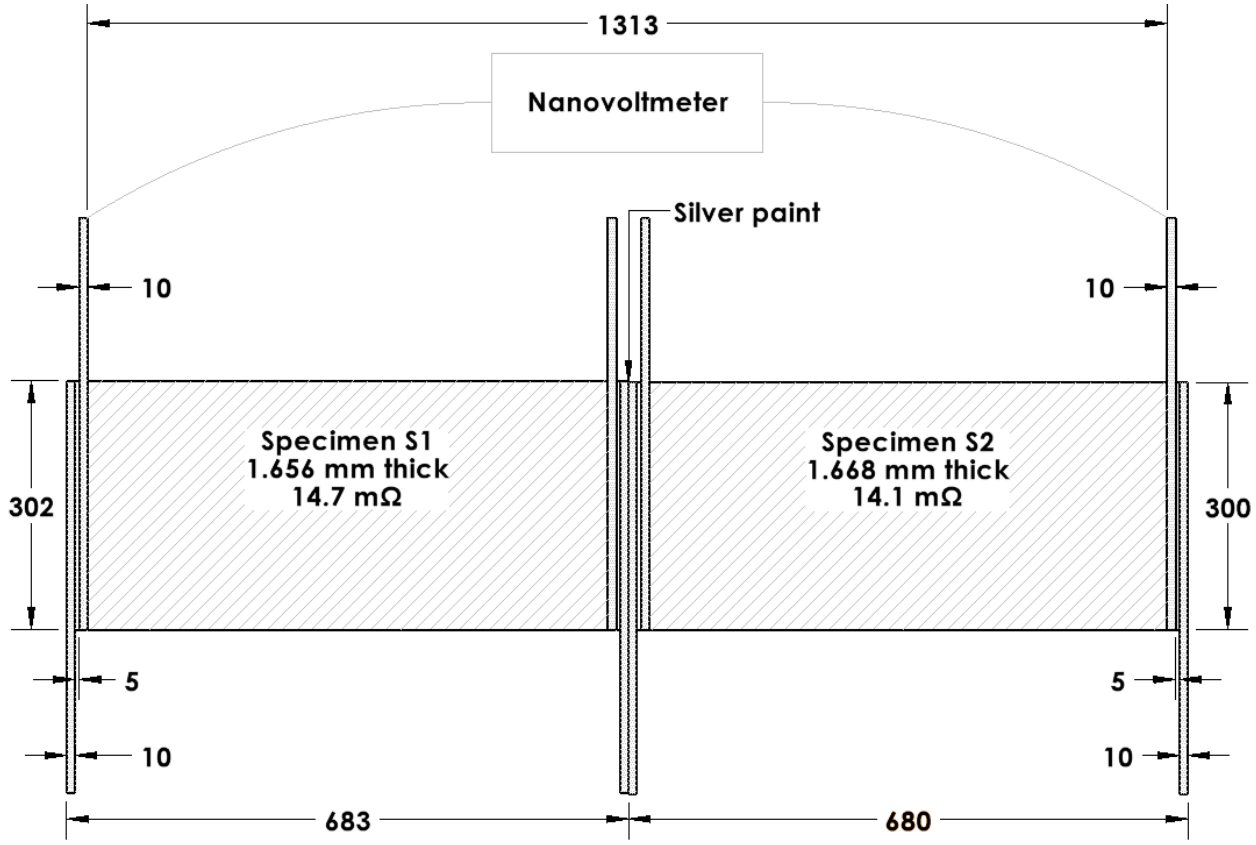

(**a**)

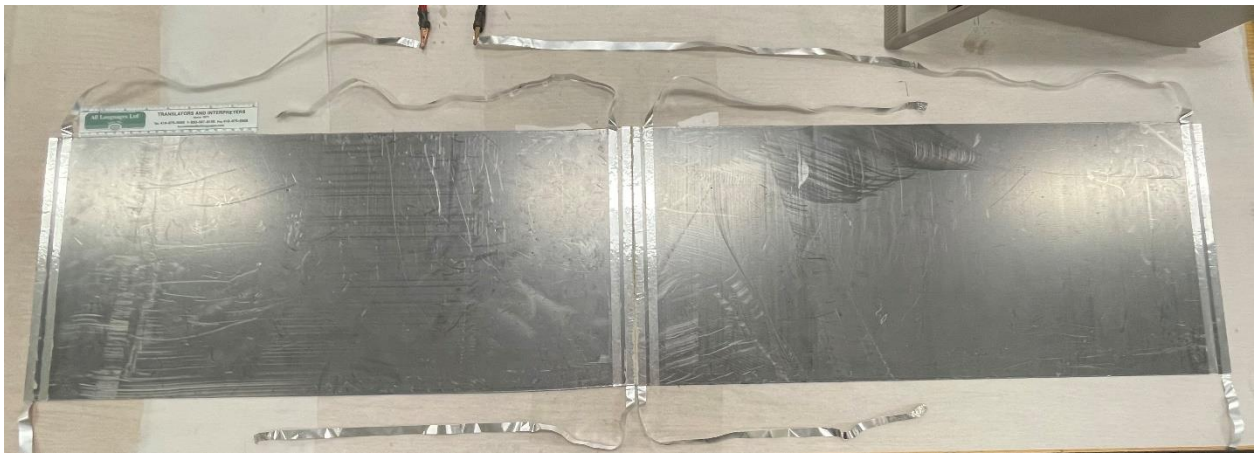

(**b**)

Figure 5. Configurations for the testing of electrets in the form of flexible graphite. Two specimens (labeled S1 and S2, Table 1) are electrically connected in series. The connection involves silver paint applied to the proximate edges of the two specimens so that the connection between the two specimens is not bent. (**a**) Schematic illustration (dimensions in mm). (**b**) Photograph with the 8-inch ruler (with divisions in inches and centimeters) having main divisions in cm in its lower scale [95].

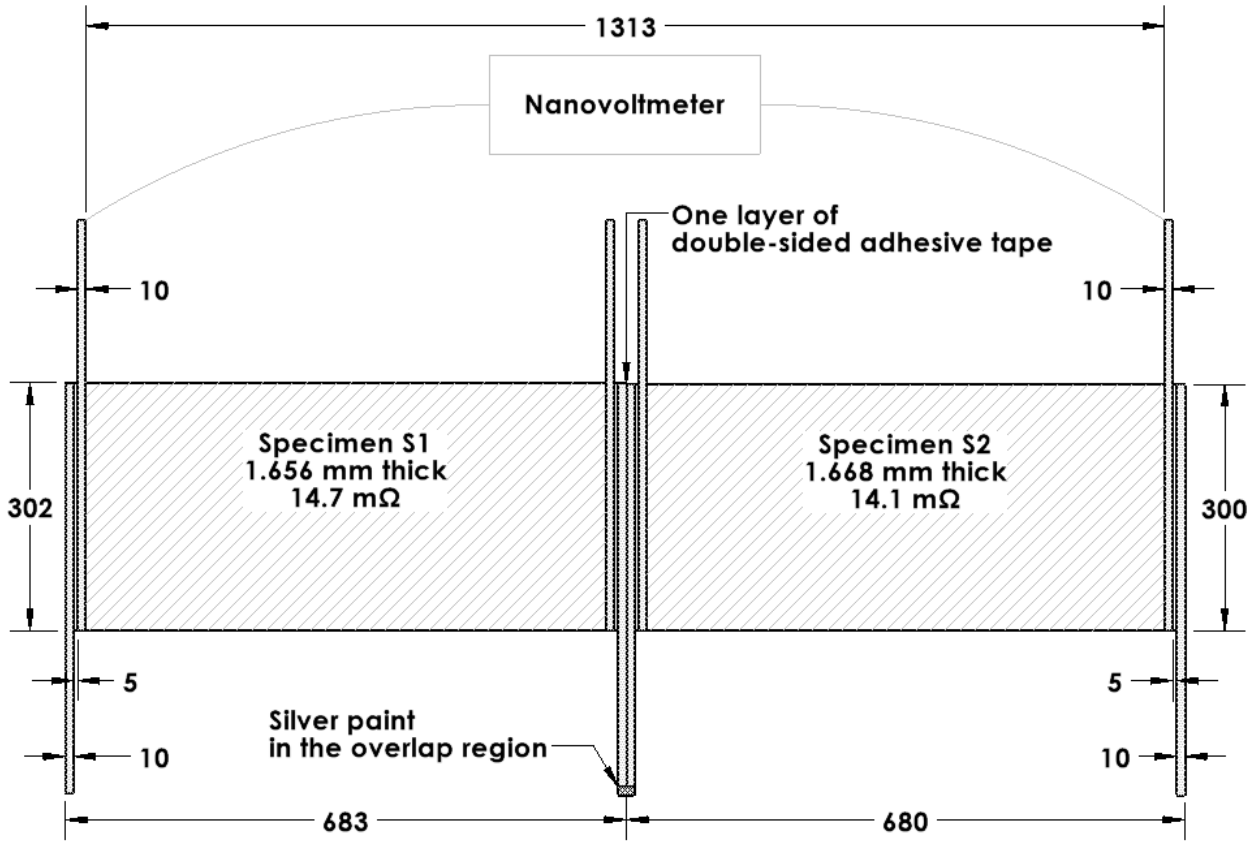

(**a**)

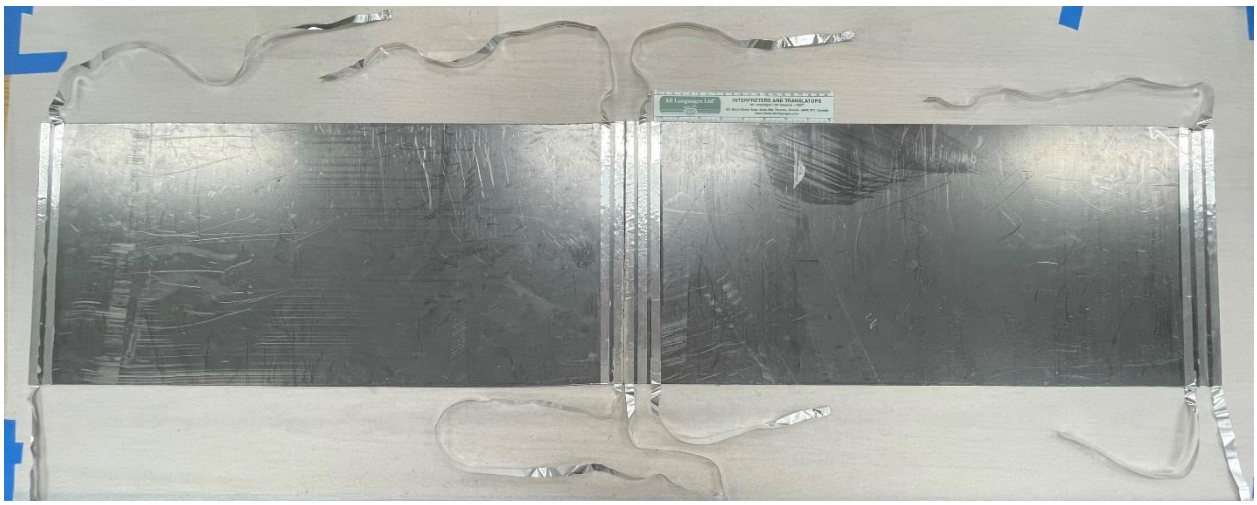

(**b**)

Figure 6. Configurations for the testing of electrets in the form of flexible graphite. Two specimens (labeled S1 and S2, Table 1) are electrically connected in series, such that they are in contact along the full length of their proximate edges, except for double-sided adhesive tape between the proximate edges. The electrical connection is achieved by using two aluminum foil electrodes that have been applied to the specimens using silver paint, which is applied near the proximate edges of the two specimens. The foils protrude from the specimens and are connected by using silver paint. As a result of the protruded part of the foil, there is much bending (curling) in the connection. (**a**) Schematic illustration (dimensions in mm). (**b**) Photograph with the 8-inch ruler (with divisions in inches and centimeters) having main divisions in cm in its lower scale [95].

Due to the electret voltage, current passes through a series of load resistances in accordance with Ohm's Law (Table 3, Figure 7) This supports the possibility of using the electret as a power source [95].

Table 3. Comparison of the measured and calculated values of the voltage across a load resistor. A flexible graphite specimen (a single piece, S1, Table 1) is in series with the load resistor [95].

Resistor Resistance (Ω)	Measured Voltage (μV)		Calculated Voltage (μV)		Current (μA)	
	Before Polarity Reversal	After Polarity Reversal	Before Polarity Reversal	After Polarity Reversal	Before Polarity Reversal	After Polarity Reversal
∞ *	+1.139 ±0.010	−0.961 ±0.009	/	/	/	/
10.000	+1.082 ±0.005	−0.911 ±0.018	+1.090 ±0.010	−0.920 ±0.009	+0.109 ±0.001	−0.092 ±0.002
1.000	+0.772 ±0.007	−0.628 ±0.003	+0.787 ±0.007	−0.664 ±0.007	+0.787 ±0.007	−0.664 ±0.006
0.1000	+0.210 ±0.005	−0.164 ±0.005	+0.208 ±0.002	−0.176 ±0.002	+2.080 ±0.018	−1.760 ± 0.017

* Open-circuit condition.

Figure 7. Testing an electret in the form of flexible graphite electrically connected to a load resistor (0.1000 Ω, shown in the bottom region of the image). The specimen is the one labeled S1 (Table 1) [95].

The electret material is preferably not bent, as the bending would decrease the voltage because of the reduction in the degree of polarization continuity [95]. Polarization continuity is an emerging concept in the field of the dielectric properties of materials. This is because nonconductive materials that dominate the study of dielectric behavior are investigated in thin dimensions along the capacitance direction and the thin dimensions do not allow variations along the thickness direction for the purpose of studying the polarization continuity [96–99].

5. Conclusions

This is the first review of the emerging subject of conductive electrets (metals and carbons without poling), which provide a new avenue for low-power electronics. Electrets provide multiple electrical functions, namely, serving as power sources and providing capacitance and resistance, with the functions being tunable via the dimensions (both length and cross-sectional area) of the electret material.

Electrets provide a low-DC current voltage (μV) while allowing a low DC (μA) to pass through. Ohm's Law is obeyed. The voltage scales with the inter-electrode distance. Series connection of multiple electret components is effective if there is no bending at the electrical connection between the components, giving a series voltage equal to the sum of the voltages of the components. In the case of bending at the electrical connection, the series voltage is below the sum. Bending within a component also diminishes the voltage because of the decrease in the degree of polarization continuity.

The science is fundamentally different from that of all previously reported power sources. The electret originates from the interaction of a tiny fraction of the carriers with the atoms. This interaction results in the charge in the electret. Dividing the electret charge by the electret voltage V' gives the electret-based capacitance C', which is higher than the permittivity-based capacitance (conventional) by orders of magnitude. Both V' and permittivity depend on the microstructure, with the values increasing with decreasing grain size. The C' governs the electret energy ($1/2\ C'V'^2$) and electret discharge time constant (RC', where R = resistance), as shown for metals. The discharge time increases with increasing inter-electrode distance. Electret discharge occurs upon short-circuiting and charges back upon subsequent open-circuiting. The discharge/charge of the electret involves that of C'.

Low-power power sources in the form of conductive electrets constitute a new field of science. This review focuses on emerging new science. The attraction of this new technology is that poling is not required and the electret materials (whether carbons or metals) are widely available. Moreover, because of the absence of any chemical reaction and the established wide utilization of the materials in structures (e.g., steel structures), there is no environmental issue. In fact, existing structures (as opposed to new structures) may be used as power sources. The electret voltage scales with the dimensions, so large structures are preferred. Because existing large structures are abundant in almost any city, large structures such as the steel rebars in a building may be used as power sources. This would involve applying electrodes to each piece (e.g., each rebar) of the structure. By staggering the discharge start time for different pieces of electret material in the same structure, continuous energy generation by the structure may be feasible. Thus, no energy storage is needed, in contrast to this need for wind and solar forms of energy. Both the common availability of electret materials and the absence of the need for energy storage are advantageous from the cost viewpoint. However, the very low power is a disadvantage, though it is expected to increase with the dimensions and with microstructural refinement, which enhances the abundance of sites for the carrier–atom interaction that is required for the polarization. As the emerging field progresses, the power is expected to increase.

Funding: This research received no funding.

Institutional Review Board Statement: Not applicable.

Informed Consent Statement: Not applicable.

Data Availability Statement: Please refer to the original cited papers for the data availability, since this is a review paper.

Conflicts of Interest: The authors declare no conflict of interest.

References

1. Lin, X.; Yang, W.; Wang, K.L.; Zhao, W. Two-dimensional spintronics for low-power electronics. *Nat. Electron.* **2019**, *2*, 274–283. [CrossRef]
2. Heo, J.; Byun, K.-E.; Lee, J.; Chung, H.-J.; Jeon, S.; Park, S.; Hwang, S. Graphene and Thin-Film Semiconductor Heterojunction Transistors Integrated on Wafer Scale for Low-Power Electronics. *Nano Lett.* **2013**, *13*, 5967–5971. [CrossRef] [PubMed]
3. Yan, X.; Cao, G.; Wang, J.; Man, M.; Zhao, J.; Zhou, Z.; Wang, H.; Pei, Y.; Wang, K.; Gao, C.; et al. Memristors based on multilayer graphene electrodes for implementing a low-power neuromorphic electronic synapse. *J. Mater. Chem. C Mater. Opt. Electron. Devices* **2020**, *8*, 4926–4933. [CrossRef]
4. Winfield, J.; Chambers, L.D.; Stinchcombe, A.; Rossiter, J.; Ieropoulos, I. The power of glove: Soft microbial fuel cell for low-power electronics. *J. Power Sources* **2014**, *249*, 327–332. [CrossRef]
5. Fanciulli, C.; Abedi, H.; Merotto, L.; Dondè, R.; De Iuliis, S.; Passaretti, F. Portable thermoelectric power generation based on catalytic combustor for low power electronic equipment. *Appl. Energy* **2018**, *215*, 300–308. [CrossRef]
6. Yeh, N.; Chiu, P.; Chyi, J.; Ren, F.; Pearton, S.J. Sb-based semiconductors for low power electronics. *J. Mater. Chem. C Mater. Opt. Electron. Devices* **2013**, *1*, 4616–4627. [CrossRef]
7. Das, S.; Prakash, A.; Salazar, R.; Appenzeller, J. Toward Low-Power Electronics: Tunneling Phenomena in Transition Metal Dichalcogenides. *ACS Nano* **2014**, *8*, 1681–1689. [CrossRef]
8. Lee, M.H.; Wei, Y.-T.; Chu, K.-Y.; Huang, J.-J.; Chen, C.-W.; Cheng, C.-C.; Chen, M.-J.; Lee, H.-Y.; Chen, Y.-S.; Lee, L.-H.; et al. Steep Slope and Near Non-Hysteresis of FETs With Antiferroelectric-Like HfZrO for Low-Power Electronics. *IEEE Electron Device Lett.* **2015**, *36*, 294–296. [CrossRef]
9. Sahu, M.; Hajra, S.; Lee, K.; Deepti, P.; Mistewicz, K.; Kim, H. Piezoelectric Nanogenerator Based on Lead-Free Flexible PVDF-Barium Titanate Composite Films for Driving Low Power Electronics. *Crystals* **2021**, *11*, 85. [CrossRef]
10. He, N.; Zhang, Q.; Tao, L.; Chen, X.; Qin, Q.; Liu, X.; Lian, X.; Wan, X.; Hu, E.; Xu, J.; et al. V_2C-Based Memristor for Applications of Low Power Electronic Synapse. *IEEE Electron Device Lett.* **2021**, *42*, 319–322. [CrossRef]
11. Torricelli, F.; Ghittorelli, M.; Smits, E.C.P.; Roelofs, C.W.S.; Janssen, R.A.J.; Gelinck, G.H.; Kovács-Vajna, Z.M.; Cantatore, E. Ambipolar Organic Tri-Gate Transistor for Low-Power Complementary Electronics. *Adv. Mater.* **2015**, *28*, 284–290. [CrossRef] [PubMed]
12. Song, Y.; Chen, X.-X.; Zhang, J.-X.; Cheng, X.-L.; Zhang, H.-X. Freestanding Micro-Supercapacitor with Interdigital Electrodes for Low-Power Electronic Systems. *J. Microelectromech. Syst.* **2017**, *26*, 1055–1062. [CrossRef]
13. Yang, Y.; Du, H.; Xue, Q.; Wei, X.; Yang, Z.; Xu, C.; Lin, D.; Jie, W.; Hao, J. Three-terminal memtransistors based on two-dimensional layered gallium selenide nanosheets for potential low-power electronics applications. *Nano Energy* **2018**, *57*, 566–573. [CrossRef]
14. Bergeron, H.; Sangwan, V.K.; McMorrow, J.J.; Campbell, G.P.; Balla, I.; Liu, X.; Bedzyk, M.J.; Marks, T.J.; Hersam, M.C. Chemical vapor deposition of monolayer MoS_2 directly on ultrathin Al_2O_3 for low-power electronics. *Appl. Phys. Lett.* **2017**, *110*, 053101. [CrossRef]
15. Rahi, S.B.; Tayal, S.; Upadhyay, A.K. A review on emerging negative capacitance field effect transistor for low power electronics. *Microelectron. J.* **2021**, *116*, 105242. [CrossRef]
16. Rani, S.; Kumar, N.; Tandon, A.; Sharma, Y. Fabrication of Binder-Free TiO_2 Nanofiber Electrodes via Electrophoretic Deposition for Low-Power Electronic Applications. *IEEE Trans. Electron Devices* **2020**, *68*, 251–256. [CrossRef]
17. Moon, H.; Seong, H.; Shin, W.C.; Park, W.-T.; Kim, M.; Lee, S.; Bong, J.H.; Noh, Y.-Y.; Cho, B.J.; Yoo, S.; et al. Synthesis of ultrathin polymer insulating layers by initiated chemical vapour deposition for low-power soft electronics. *Nat. Mater.* **2015**, *14*, 628–635. [CrossRef]
18. Kim, K.; Jung, M.; Kim, B.; Kim, J.; Shin, K.; Kwon, O.-S.; Jeon, S. Low-voltage, high-sensitivity and high-reliability bimodal sensor array with fully inkjet-printed flexible conducting electrode for low power consumption electronic skin. *Nano Energy* **2017**, *41*, 301–307. [CrossRef]
19. Sullivan, P.; Schumann, S.; Da Campo, R.; Howells, T.; Duraud, A.; Shipman, M.; Hatton, R.A.; Jones, T.S. Ultra-high voltage multijunction organic solar cells for low-power electronic applications. *Adv. Energy Mater.* **2013**, *3*, 239–244. [CrossRef]
20. Mohanta, M.K.; Fathima, I.S.; De Sarkar, A. Exceptional mechano-electronic properties in the HfN2 monolayer: A promising candidate in low-power flexible electronics, memory devices and photocatalysis. *Phys. Chem. Chem. Phys.* **2020**, *22*, 21275–21287. [CrossRef]
21. Khushboo; Azad, P. A triboelectric energy harvester using human biomechanical motion for low power electronics. *Bull. Mater. Sci.* **2019**, *42*, 121. [CrossRef]
22. Uzun, Y. Design and Implementation of RF Energy Harvesting System for Low-Power Electronic Devices. *J. Electron. Mater.* **2016**, *45*, 3842–3847. [CrossRef]
23. Cunha, I.; Ferreira, S.H.; Martins, J.; Fortunato, E.; Gaspar, D.; Martins, R.; Pereira, L. Foldable and Recyclable Iontronic Cellulose Nanopaper for Low-Power Paper Electronics. *Adv. Sustain. Syst.* **2022**, *6*, 2200177. [CrossRef]
24. Park, S.Y.; Heo, J.; Yoon, Y.J.; Kim, J.W.; Jang, H.; Walker, B.; Kim, J.Y. Synergistic combination of amorphous indium oxide with tantalum pentoxide for efficient electron transport in low-power electronics. *J. Mater. Chem. C* **2019**, *7*, 4559–4566. [CrossRef]
25. Heo, J.; Park, S.Y.; Kim, J.W.; Song, S.; Yoon, Y.J.; Jeong, J.; Jang, H.; Lee, K.T.; Seo, J.H.; Walker, B.; et al. Implementation of Low-Power Electronic Devices Using Solution-Processed Tantalum Pentoxide Dielectric. *Adv. Funct. Mater.* **2018**, *28*, 1704215. [CrossRef]

26. Erhard, D.P.; Lovera, D.; von Salis-Soglio, C.; Giesa, R.; Altstädt, V.; Schmidt, H.-W. Recent Advances in the Improvement of Polymer Electret Films. *Adv. Polym. Sci.* **2010**, *228*, 155–207. [CrossRef]
27. Pillai, P.K.C. Polymeric electrets. *Plast. Eng.* **1995**, *28*, 1–61.
28. Sessler, G.M. Electrets: Recent developments. *J. Electrost.* **2001**, *51–52*, 137–145. [CrossRef]
29. Kressmann, R.; Sessler, G.M.; Guenther, P. Space-charge electrets. *IEEE Trans Dielectr. Electr. Insul.* **1996**, *3*, 607–623. [CrossRef]
30. Liu, Y.-C.; Aoyagi, Y.; Chung, D.D.L. Development of epoxy-based electrets. *J. Mater. Sci.* **2008**, *43*, 1650–1663. [CrossRef]
31. Huang, C.-Y.; Chung, D. Controlling and increasing the inherent voltage in cement paste. *Adv. Cem. Res.* **2009**, *21*, 31–37. [CrossRef]
32. Lindner, M.; Hoislbauer, H.; Schwodiauer, R.; Bauer-Gogonea, S.; Bauer, S. Charged cellular polymers with "ferroelectretic" behavior. *IEEE Trans. Dielectr. Electr. Insul.* **2004**, *11*, 255–263. [CrossRef]
33. Chen, C.-H.; Wang, Y.; Michinobu, T.; Chang, S.-W.; Chiu, Y.-C.; Ke, C.-Y.; Liou, G.-S. Donor–Acceptor Effect of Carbazole-Based Conjugated Polymer Electrets on Photoresponsive Flash Organic Field-Effect Transistor Memories. *ACS Appl. Mater. Interfaces* **2020**, *12*, 6144–6150. [CrossRef]
34. Sano, C.; Ataka, M.; Hashiguchi, G.; Toshiyoshi, H. An Electret-Augmented Low-Voltage MEMS Electrostatic Out-of-Plane Actuator for Acoustic Transducer Applications. *Micromachines* **2020**, *11*, 267. [CrossRef] [PubMed]
35. Sano, C.; Menon, V.; Honma, H.; Hashiguchi, G.; Toshiyoshi, H. Low-voltage-driven electrostatic microspeakers with potassium-ion-electrets. *J. Physics Conf. Series* **2019**, *1407*, 012129. [CrossRef]
36. Li, Z.B.; Li, H.Y.; Fan, Y.J.; Liu, L.; Chen, Y.H.; Zhang, C.; Zhu, G. Small-sized, lightweight, and flexible triboelectric nano-generator enhanced by PTFE/PDMS nanocomposite electret. ACS Applied Mater. *Interfaces* **2019**, *11*, 20370–20377.
37. Shih, C.-C.; Chiang, Y.-C.; Hsieh, H.-C.; Lin, Y.-C.; Chen, W.-C. Multilevel Photonic Transistor Memory Devices Using Conjugated/Insulated Polymer Blend Electrets. *ACS Appl. Mater. Interfaces* **2019**, *11*, 42429–42437. [CrossRef]
38. Cheng, S.-W.; Han, T.; Huang, T.-Y.; Chien, Y.-H.C.; Liu, C.-L.; Tang, B.Z.; Liou, G.-S. Novel Organic Phototransistor-Based Nonvolatile Memory Integrated with UV-Sensing/Green-Emissive Aggregation Enhanced Emission (AEE)-Active Aromatic Polyamide Electret Layer. *ACS Appl. Mater. Interfaces* **2018**, *10*, 18281–18288. [CrossRef]
39. Zhou, T.; Zhang, L.; Xue, F.; Tang, W.; Zhang, C.; Wang, Z.L. Multilayered electret films based triboelectric nanogenerator. *Nano Res.* **2016**, *9*, 1442–1451. [CrossRef]
40. Tung, W.-Y.; Li, M.-H.; Wu, H.-C.; Liu, H.-Y.; Hsieh, Y.-T.; Chen, W.-C. High Performance Nonvolatile Transistor Memories Utilizing Functional Polyimide-Based Supramolecular Electrets. *Chem. Asian J.* **2016**, *11*, 1631–1640. [CrossRef]
41. Shibata, Y.; Sugiyama, T.; Mimura, H.; Hashiguchi, G. In Situ Measurement of Charging Process in Electret-Based Comb-Drive Actuator and High-Voltage Charging. *J. Microelectromech. Syst.* **2014**, *24*, 1052–1060. [CrossRef]
42. Lu, G.; Koch, N.; Neher, D. In-situ tuning threshold voltage of field-effect transistors based on blends of poly(3-hexylthiophene) with an insulator electret. *Appl. Phys. Lett.* **2015**, *107*, 063301. [CrossRef]
43. Shih, C.-C.; Chiu, Y.-C.; Lee, W.-Y.; Chen, J.-Y.; Chen, W.-C. Conjugated Polymer Nanoparticles as Nano Floating Gate Electrets for High Performance Nonvolatile Organic Transistor Memory Devices. *Adv. Funct. Mater.* **2015**, *25*, 1511–1519. [CrossRef]
44. Yang, Y.; Zhang, H.; Zhong, X.; Yi, F.; Yu, R.; Zhang, Y.; Wang, Z.L. Electret Film-Enhanced Triboelectric Nanogenerator Matrix for Self-Powered Instantaneous Tactile Imaging. *ACS Appl. Mater. Interfaces* **2014**, *6*, 3680–3688. [CrossRef] [PubMed]
45. Thakur, R.; Das, D.; Das, A. Study of charge decay in corona-charged fibrous electrets. *Fibers Polym.* **2014**, *15*, 1436–1443. [CrossRef]
46. Feng, Y.; Hagiwara, K.; Iguchi, Y.; Suzuki, Y. Trench-filled cellular parylene electret for piezoelectric transducer. *Appl. Phys. Lett.* **2012**, *100*, 262901. [CrossRef]
47. Paajanen, M.; Lekkala, J.; Kirjavainen, K. ElectroMechanical Film (EMFi)—A new multipurpose electret material. *Sens. Actuators A Phys.* **2000**, *84*, 95–102. [CrossRef]
48. Rychkov, A.; Kuznetsov, A.; Gulyakova, A.; Rychkov, D. Surface Potential Decay of Corona Charged Polyethylene Films: Influence of Deep Surface Traps. *IEEE Trans. Dielectr. Electr. Insul.* **2021**, *28*, 1933–1937. [CrossRef]
49. Wang, J.; Rychkov, D.; Nguyen, Q.D.; Gerhard, R. Unexpected bipolar space-charge polarization across transcrystalline interfaces in polypropylene electret films. *J. Appl. Phys.* **2020**, *128*, 134103. [CrossRef]
50. Lan, C.; Zou, H.; Wang, L.; Zhang, M.; Pan, S.; Ma, Y.; Qiu, Y.; Wang, Z.L.; Lin, Z. Revealing electrical-poling-induced po-larization potential in hybrid perovskite photodetectors. *Adv. Mater.* **2020**, *32*, 2005481. [CrossRef] [PubMed]
51. Guliakova, A.A.; Galikhanov, M.F.; Galeeva, L.R.; Gilfanova, S.V.; Fang, P. Investigation of electret and filtering properties of polypropylene-based nonwoven fabrics and its composites with 2 vol% of silicon dioxide inclusions. *IEEE Trans. Dielectr. Electr. Insul.* **2020**, *27*, 1656–1661. [CrossRef]
52. Komeijani, A.; Bagheri, H.; Shekarchi, B. Surface potential uniformity and sensitivity of large-area PTFE electret discs of different thicknesses produced by a modified corona poling rotating system for dosimetry applications. *J. Adv. Dielectr.* **2019**, *9*, 1950050. [CrossRef]
53. Sohrabi, M.; Komijani, A. Modified single point-to-plane corona poling rotating system for production of electret dosimeters. *IEEE Trans. Dielectr. Electr. Insul.* **2018**, *25*, 448–456. [CrossRef]
54. Horiuchi, N.; Madokoro, K.; Nozaki, K.; Nakamura, M.; Katayama, K.; Nagai, A.; Yamashita, K. Electrical conductivity of polycrystalline hydroxyapatite and its application to electret formation. *Solid State Ion.* **2018**, *315*, 19–25. [CrossRef]

55. Zhang, J.W.; Gao, F.K.; Sun, H.C.; Putson, C.; Liu, R.T. Electrostrictive energy conversion property of cellular electrets after corona discharge. *Int. J. Mod. Phys. B* **2018**, *32*, 1850069. [CrossRef]
56. Ko, Y.S.; Nüesch, F.A.; Opris, D.M. Charge generation by ultra-stretchable elastomeric electrets. *J. Mater. Chem. C* **2017**, *5*, 1826–1835. [CrossRef]
57. Xi, X.; Chung, D. Electret, piezoelectret, dielectricity and piezoresistivity discovered in exfoliated-graphite-based flexible graphite, with applications in mechanical sensing and electric powering. *Carbon* **2019**, *150*, 531–548. [CrossRef]
58. Xi, X.; Chung, D.D.L. Dielectric behavior of graphite, with assimilation of the AC permittivity, DC polarization and DC electret. *Carbon* **2021**, *181*, 246–259. [CrossRef]
59. Xi, X.; Chung, D. Electret behavior of unpoled carbon fiber with and without nickel coating. *Carbon* **2019**, *159*, 122–132. [CrossRef]
60. Xi, X.; Chung, D. Electret behavior of carbon fiber structural composites with carbon and polymer matrices, and its application in self-sensing and self-powering. *Carbon* **2020**, *160*, 361–389. [CrossRef]
61. Xi, X.; Chung, D.D.L. Electret, piezoelectret and piezoresistivity discovered in steels, with application to structural self-sensing and structural self-powering. *Smart Mater. Struct.* **2019**, *28*, 075028. [CrossRef]
62. Yang, W.; Chung, D.D.L. Electret behavior discovered in solder, specifically tin–silver. *J. Mater. Sci. Mater. Electron.* **2021**, *32*, 19145–19156. [CrossRef]
63. David, I.G.; Popa, D.-E.; Buleandra, M. Pencil Graphite Electrodes: A Versatile Tool in Electroanalysis. *J. Anal. Methods Chem.* **2017**, *2017*, 1905968. [CrossRef]
64. Billaud, J.; Bouville, F.; Magrini, T.; Villevieille, C.; Studart, A.R. Magnetically aligned graphite electrodes for high-rate performance Li-ion batteries. *Nat. Energy* **2016**, *1*, 16097. [CrossRef]
65. Bhauriyal, P.; Mahata, A.; Pathak, B. The staging mechanism of $AlCl_4$ intercalation in a graphite electrode for an aluminiumion battery. *Phys. Chem. Chem. Phys.* **2017**, *19*, 7980–7989. [CrossRef] [PubMed]
66. Fan, L.; Liu, Q.; Chen, S.; Lin, K.; Xu, Z.; Lu, B. Potassium-Based Dual Ion Battery with Dual-Graphite Electrode. *Small* **2017**, *13*, 1701011. [CrossRef] [PubMed]
67. Fan, H.; Qi, L.; Wang, H. Hexafluorophosphate anion intercalation into graphite electrode from methyl propionate. *Solid State Ion.* **2017**, *300*, 169–174. [CrossRef]
68. Cai, W.; Yan, C.; Yao, Y.; Xu, L.; Chen, X.; Huang, J.; Zhang, Q. The Boundary of Lithium Plating in Graphite Electrode for Safe Lithium-Ion Batteries. *Angew. Chem. Int. Ed.* **2021**, *60*, 13007–13012. [CrossRef] [PubMed]
69. Finegan, D.P.; Quinn, A.; Wragg, D.S.; Colclasure, A.M.; Lu, X.; Tan, C.; Heenan, T.M.M.; Jervis, R.; Brett, D.J.L.; Das, S.; et al. Spatial dynamics of lithiation and lithium plating during high-rate operation of graphite electrodes. *Energy Environ. Sci.* **2020**, *13*, 2570–2584. [CrossRef]
70. Patil, M.M.; Shetti, N.P.; Malode, S.J.; Nayak, D.S.; Chakklabbi, T.R. Electroanalysis of paracetamol at nanoclay modified graphite electrode. *Mater. Today Proc.* **2019**, *18*, 986–993. [CrossRef]
71. Zhu, S.; Zhang, L.; Huang, Y.; Li, J.; Fan, H.; Wang, H. Ethylmethyl carbonate's role in hexafluor-ophosphate storage in graphite electrodes. *ACS Appl. Energy Mater.* **2019**, *2*, 8031–8038. [CrossRef]
72. Goktas, M.; Bolli, C.; Buchheim, J.; Berg, E.J.; Novák, P.; Bonilla, F.; Rojo, T.; Komaba, S.; Kubota, K.; Adelhelm, P. Stable and Unstable Diglyme-Based Electrolytes for Batteries with Sodium or Graphite as Electrode. *ACS Appl. Mater. Interfaces* **2019**, *11*, 32844–32855. [CrossRef] [PubMed]
73. Hogrefe, C.; Hein, S.; Waldmann, T.; Danner, T.; Richter, K.; Latz, A.; Wohlfahrt-Mehrens, M. Mechanistic Details of the Spontaneous Intercalation of Li Metal into Graphite Electrodes. *J. Electrochem. Soc.* **2020**, *167*, 140546. [CrossRef]
74. Zhang, L.; Li, J.; Huang, Y.; Zhu, D.; Wang, H. Synergetic Effect of ethyl methyl carbonate and trime-thyl phosphate on BF4-intercalation into a graphite electrode. *Langmuir* **2019**, *35*, 3972–3979. [CrossRef]
75. Sharma, S.; Jain, R.; Raja, A.N. Review-pencil graphite electrode: An emerging sensing material. *J. Electrochem. Soc.* **2020**, *167*, 037501.
76. Huang, Y.; Fan, H.; Kamezaki, H.; Kang, B.; Yoshio, M.; Wang, H. Facilitating Tetrafluoroborate Intercalation into Graphite Electrodes from Ethylmethyl Carbonate-Based Solutions. *Chemelectrochem* **2019**, *6*, 2931–2936. [CrossRef]
77. Morasch, R.; Landesfeind, J.; Suthar, B.; Gasteiger, H. Detection of Binder Gradients Using Impedance Spectroscopy and Their Influence on the Tortuosity of Li-Ion Battery Graphite Electrodes. *J. Electrochem. Soc.* **2018**, *165*, A3459–A3467. [CrossRef]
78. Amin, R.; Delattre, B.; Tomsia, A.P.; Chiang, Y.-M. Electrochemical Characterization of High Energy Density Graphite Electrodes Made by Freeze-Casting. *ACS Appl. Energy Mater.* **2018**, *1*, 4976–4981. [CrossRef]
79. Liu, L.; Solin, N.; Inganäs, O. Scalable lignin/graphite electrodes formed by mechanochemistry. *RSC Adv.* **2019**, *9*, 39758–39767. [CrossRef]
80. Chung, D.; Xi, X. A review of the colossal permittivity of electronic conductors, specifically metals and carbons. *Mater. Res. Bull.* **2021**, *148*, 111654. [CrossRef]
81. Chung, D.; Xi, X. Factors that govern the electric permittivity of carbon materials in the graphite allotrope family. *Carbon* **2021**, *184*, 245–252. [CrossRef]
82. Jonscher, A.K. Dielectric relaxation in solids. *J. Phys. D Appl. Phys.* **1999**, *32*, R57–R70. [CrossRef]
83. Chung, D.; Xi, X. Electric poling of carbon fiber with and without nickel coating. *Carbon* **2020**, *162*, 25–35. [CrossRef]
84. Chung, D.D.L.; Xi, X. New concept of electret-based capacitance, as shown for solder and other conductors. *J. Mater. Sci. Mater. Electron.* **2022**, *33*, 27022–27039. [CrossRef]

85. Chung, D.D.L.; Xi, X. Introducing solder-based electronics, with solder functioning as resistor, capacitor, and power source. *J. Mater. Sci. Mater. Electron.* **2023**, *34*, 131. [CrossRef]
86. Chung, D.D.L. A review of exfoliated graphite. *J. Mater. Sci.* **2015**, *51*, 554–568. [CrossRef]
87. Xin, G.; Wang, Y.; Liu, X.; Zhang, J.; Wang, Y.; Huang, J.; Zang, J. Preparation of self-supporting graphene on flexible graphite sheet and electrodeposition of polyaniline for supercapacitor. *Electrochim. Acta* **2015**, *167*, 254–261. [CrossRef]
88. Sykam, N.; Rao, G.M. Lightweight flexible graphite sheet for high-performance electromagnetic interference shielding. *Mater. Lett.* **2018**, *233*, 59–62. [CrossRef]
89. Liu, Y.; Zeng, J.; Han, D.; Wu, K.; Yu, B.; Chai, S.; Chen, F.; Fu, Q. Graphene enhanced flexible expanded graphite film with high electric, thermal conductivities and EMI shielding at low content. *Carbon* **2018**, *133*, 435–445. [CrossRef]
90. Muniraj VK, A.; Dwivedi, P.K.; Tamhane, P.S.; Szunerits, S.; Boukherroub, R.; Shelke, M.V. High-energy flexible supercapacitor-synergistic effects of polyhydroquinone and $RuO_2 \cdot \times H_2O$ with microsized, few-layered, self-supportive exfoliated-graphite sheets. *ACS Appl. Mater. Interfaces* **2019**, *11*, 18349–18360. [CrossRef] [PubMed]
91. Liu, Y.; Zhang, K.; Mo, Y.; Zhu, L.; Yu, B.; Chen, F.; Fu, Q. Hydrated aramid nanofiber network enhanced flexible expanded graphite films towards high EMI shielding and thermal properties. *Compos. Sci. Technol.* **2018**, *168*, 28–37. [CrossRef]
92. Goren, A.Y.; Recepoğlu, Y.K.; Edebalï, O.; Sahin, C.; Genisoglu, M.; Okten, H.E. Electrochemical Degradation of Methylene Blue by a Flexible Graphite Electrode: Techno-Economic Evaluation. *ACS Omega* **2022**, *7*, 32640–32652. [CrossRef] [PubMed]
93. Li, H.-Y.; Yu, Y.; Liu, L.; Liu, L.; Wu, Y. One-step electrochemically expanded graphite foil for flexible all-solid supercapacitor with high rate performance. *Electrochim. Acta* **2017**, *228*, 553–561. [CrossRef]
94. Liu, Y.; Qu, B.; Wu, X.; Tian, Y.; Wu, K.; Yu, B.; Du, R.; Fu, Q.; Chen, F. Utilizing ammonium persulfate assisted expansion to fabricate flexible expanded graphite films with excellent thermal conductivity by introducing wrinkles. *Carbon* **2019**, *153*, 565–574. [CrossRef]
95. Chung, D.; Duong, D.Q. Observation of electric polarization continuity in graphite. *Mater. Chem. Phys.* **2023**, *297*, 127357. [CrossRef]
96. Ukpaka, C.P. Mathematical model to predict the characteristics of polarization in dielectric materials: The concept of piezoelectrcity and electrostriction. *Chem. Int.* **2019**, *5*, 232–240.
97. Zhang, G.; Brannum, D.; Dong, D.; Tang, L.; Allahyarov, E.; Tang, S.; Kodweis, K.; Lee, J.-K.; Zhu, L. Interfacial Polarization-Induced Loss Mechanisms in Polypropylene/$BaTiO_3$ Nanocomposite Dielectrics. *Chem. Mater.* **2016**, *28*, 4646–4660. [CrossRef]
98. Quan, B.; Liang, X.; Ji, G.; Cheng, Y.; Liu, W.; Ma, J.; Zhang, Y.; Li, D.; Xu, G. Dielectric polarization in electromagnetic wave absorption: Review and perspective. *J. Alloys Compd.* **2017**, *728*, 1065–1075. [CrossRef]
99. Kim, M.P.; Um, D.-S.; Shin, Y.-E.; Ko, H. High-Performance Triboelectric Devices via Dielectric Polarization: A Review. *Nanoscale Res. Lett.* **2021**, *16*, 35. [CrossRef]